Pancreatic Cancer Organoids from the Human Cancer Models Initiative Biobank Reflect Disease Genotypes, Capture Patient Heterogeneity, and are Amenable to Therapeutic Screening

Stephen Friend, MS; Matthew Graziano, BS; Rachel Demerath, MS; and James Clinton, PhD
ATCC®, Manassas, VA 20110

ATCC®
Credible leads to Incredible™

Abstract 4239

Introduction

- Pancreatic cancer is the fourth leading cause of cancer-related death in the United States (~3% of all cancer cases) and has one of the lowest 5-year relative survival rates.
- There is a lack of clinically representative, easily available, validated, in vitro pancreatic cancer models that reflect the genomic and phenotypic diversity of the disease.
- The Human Cancer Models Initiative (HCMI) is an international collaborative project devoted to the development and distribution of approximately 1,000 novel human primary tissue–derived tumor models supported with clinical and molecular annotation.
- ATCC® has made 300+ of these next-generation cancer models, including 50+ pancreatic cancer organoids (PCOs), available to the research community through our catalog.
- Here, we describe a subset of the pancreatic model cohort, highlight their clinical characteristics, characterize their genotype, and investigate their response to a 10-compound panel of chemotherapeutics that include taxanes, platinum compounds, KRAS-targeting inhibitors, and PARP inhibitors.

Human Cancer Models Initiative (HCMI)

HCMI is an international consortium of organizations with the shared goal of creating next-generation in vitro cancer models that better represent the diversity and complexity of human cancers than seen in existing cancer cell lines. These models are annotated with detailed clinical (e.g., patient demographics and treatment history) and molecular data (e.g., WGS, WES). These novel models are manufactured and distributed by ATCC®. Over 300 models are currently available, including 3-D cancer organoids, from 23 different primary tissue sites. Over 50 PCOs are currently available, a subset of which are described in Table 1.

Methods

Organoid culture: PCOs were sourced from ATCC® and cultured in standard extracellular matrix (ECM)-embedded conditions according to recommended protocols (Clinton et al. 2019) utilizing Organoid Growth Kit 1B (ATCC® ACS-7101™), Cell Basement Membrane (ATCC® ACS-3035™), and ROCK Inhibitor Y27632 (ATCC® ACS-3030™).

Drug response: Viability studies were performed between passages 2 and 10. Passage occurred 72 hours prior to seeding to allow single cells and cell fragments to reform small organoids prior to seeding and dosing. Organoids were collected, ECM removed, and seeded as intact organoids into white walled 96-well plates at the equivalent of ~2.5x10^3 cells/well in complete growth media supplemented with 0.5 mg/mL ECM. Compounds for the drug screening panel were KRpep-2d, MRTX1133, nab-paclitaxel, cisplatin, 5-fluorouracil (5-FU), olaparib, oxaliplatin, PJ34, paclitaxel, and rucaparib. Drugs were reconstituted in either H_2O, DMSO, or NaCl. Positive control for drug response was 200 µM cisplatin. Drug exposure and assay timepoints are shown in Figure 1. Viability was determined using the CellTiter-Glo® 3D Luminescent Cell Viability Assay (Promega®). Response was normalized to the vehicle condition and expressed as percent viability. Figures were plotted, non-linear curves generated, and IC_{50} was calculated in GraphPad Prism®. Points reflect average with SEM of 5-6 technical replicates. Z' Factor scores were determined using vehicle control and positive control.

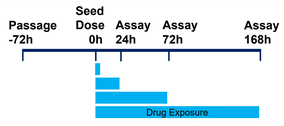

Figure 1: Summary of workflow. Preparation, dosing, and assay timepoints.

Imaging and histology: Organoids in culture were routinely monitored via brightfield microscopy. Prior to each viability assay, images were taken of each well to monitor morphology. For histology, organoids were collected, ECM removed, pelleted, fixed in 4% paraformaldehyde, embedded in paraffin, sectioned at 10 µm, mounted on slides, and stained with hematoxylin and eosin (H&E) to visualize morphology (Figure 3).

Sequencing: Organoids were collected, ECM removed, and DNA extracted using a QIAGEN® EZ1® Advanced XL instrument with an EZ1® DNA Tissue Kit. DNA concentration and purity were measured using a NanoDrop® 2000. Libraries were prepared using a targeted cancer panel (~600 genes) for hybrid capture. Sequencing was performed by Illumina® NovaSeq® 6000. Average target depth was >1300X. Low quality data were filtered, and alignment was performed against GRCh37. Variants were filtered and annotated. Oncoplot of selected key genes and variants associated with pancreatic cancer are shown in Figure 2.

Results

Table 1: Clinical characteristics of established human PCOs (n=46) from the HCMI biobank. Models were predominantly derived from primary tumors (75%), had an adenocarcinoma ductal histological subtype (PDAC, 74%), and were from patients with an average age of 65 years at diagnosis that were primarily female (56%). Highlighted models (n=4) were used in subsequent experiments.

ATCC® No.	Cancer Type	Histological Subtype	Type	Acquisition Site	Gender	Age	Clinical Stage
PDM-36™	Pancreatic	Adeno. ductal type	Primary	Pancreatic head	Male	62	Stage III
PDM-37™	Pancreatic	Squamous cell carcinoma	Primary	Pancreatic head	Female	64	Stage III
PDM-38™	Pancreatic	Adeno. ductal type	Primary	Pancreatic tail	Female	63	Stage IIB
PDM-289™	Pancreatic	Moderately differentiated Adeno.	Metastasis	Liver	Female	68	Stage IV
PDM-101™	Pancreatic	Adeno. ductal type	Primary	Pancreatic neck	Female	80	Stage IIB
PDM-110™	Pancreatic	Adeno. ductal type	Primary	Pancreatic head	Female	62	--
PDM-134™	Pancreatic	Adeno. (NOS)	Primary	Pancreatic body	Female	64	Stage IIB
PDM-137™	Pancreatic	Adeno. ductal type	Primary	Pancreatic body	Male	60	Stage IIA
PDM-138™	Pancreatic	Adeno. (NOS)	Primary	Pancreatic body	Male	72	--
PDM-197™	Pancreatic	Adeno. ductal type	Primary	Pancreatic head	Female	60	--
PDM-198™	Pancreatic	Adeno. ductal type	Primary	Pancreatic tail	Female	64	--
PDM-200™	Pancreatic	Adeno. ductal type	Primary	Pancreatic head	Female	60	--
PDM-201™	Pancreatic	Adeno. ductal type	Primary	Pancreatic head	Female	63	Stage IIB
PDM-203™	Pancreatic	Adeno. ductal type	Primary	Pancreatic tail	Male	74	--
PDM-204™	Pancreatic	Adeno. ductal type	Primary	Pancreatic tail	Female	63	Stage III
PDM-205™	Pancreatic	Adeno. ductal type	Primary	Pancreatic head	Female	77	--
PDM-24™	Pancreatic	Adeno. ductal type	Primary	Pancreatic head	Male	55	Stage III
PDM-25™	Pancreatic	Adeno. ductal type	Primary	Pancreatic head	Male	54	--
PDM-26™	Pancreatic	Adeno. ductal type	Primary	Pancreatic body	Female	74	Stage IIB
PDM-27™	Pancreatic	Adeno. ductal type	Primary	Pancreatic head	Female	74	--
PDM-270™	Pancreatic	Adeno. ductal type	Primary	Pancreatic head	Male	48	Stage IV
PDM-28™	Pancreatic	Adeno. ductal type	Primary	Pancreatic body	Male	66	Stage III
PDM-29™	Pancreatic	Infiltrating ductal carcinoma	Primary	Pancreatic head	Male	72	--

ATCC® No.	Cancer Type	Histological Subtype	Type	Acquisition Site	Gender	Age	Clinical Stage
PDM-30™	Pancreatic	Adeno. ductal type	Primary	Pancreatic head	Male	75	Stage III
PDM-31™	Pancreatic	Adeno. ductal type	Primary	Pancreatic head	Female	60	Stage III
PDM-32™	Pancreatic	Adeno. ductal type	Primary	Pancreatic head	Male	57	Stage III
PDM-33™	Pancreatic	Adeno. ductal type	Primary	Pancreatic head	Male	77	--
PDM-34™	Pancreatic	Adeno. ductal type	Primary	Pancreatic head	Female	73	--
PDM-35™	Pancreatic	Adeno. ductal type	Primary	Pancreatic head	Male	75	--
PDM-39™	Pancreatic	Adeno. ductal type	Primary	Pancreatic head	Male	69	Stage III
PDM-40™	Pancreatic	Adeno. ductal type	Primary	Pancreatic head	Female	71	Stage III
PDM-41™	Pancreatic	Adeno. ductal type	Primary	Pancreatic head	Female	61	Stage III
PDM-421™	Pancreatic	Adeno. ductal type	Primary	Pancreatic head	Male	54	Stage III
PDM-423™	Pancreatic	Adeno. ductal type	Primary	Pancreatic body	Female	67	Stage III
PDM-90™	Pancreatic	Adeno. (NOS)	Primary	Pancreas	Female	--	Stage IIA
PDM-106™	Pancreatic	Other	Metastasis	Liver	Female	63	Stage IIB
PDM-107™	Pancreatic	Adeno. ductal type	Metastasis	Liver	Female	49	Stage IIB
PDM-108™	Pancreatic	Other	Metastasis	Liver	Female	53	--
PDM-126™	Pancreatic	Adeno. (NOS)	Metastasis	Pleural cavity	Male	66	Stage IV
PDM-164™	Pancreatic	Adeno. ductal type	Metastasis	Peritoneum	Male	66	--
PDM-168™	Pancreatic	Adeno. ductal type	Metastasis	Other	Female	60	--
PDM-170™	Pancreatic	Adeno. ductal type	Metastasis	Pleural cavity	Male	73	--
PDM-179™	Pancreatic	Adeno. ductal type	Metastasis	Liver	Female	74	--
PDM-221™	Pancreatic	Infiltrating ductal carcinoma	Metastasis	Lymph node(s)	Male	72	--
PDM-222™	Pancreatic	Infiltrating ductal carcinoma	Metastasis	Pancreatic head	Male	62	--
PDM-288™	Pancreatic	Moderately differentiated Adeno.	Metastasis	Liver	Female	68	Stage IV

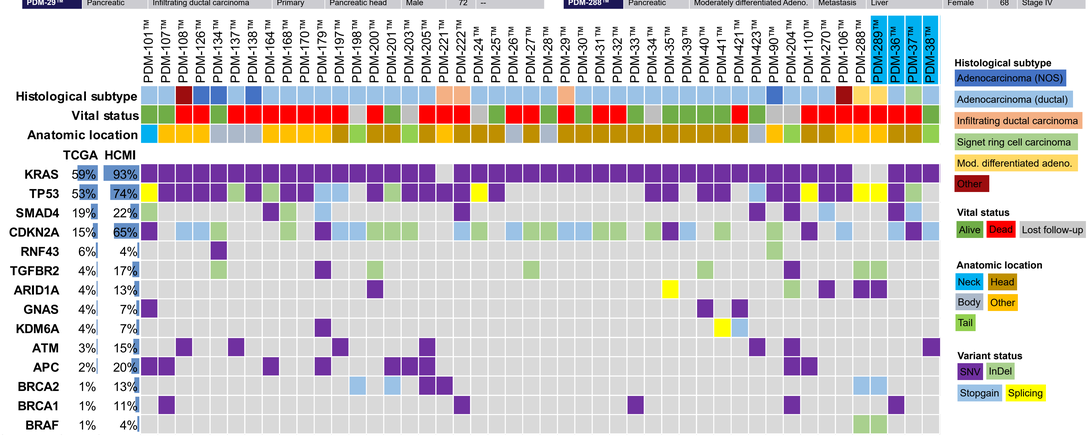

Figure 2: Oncoplot of selected somatic pancreatic cancer relevant mutations in patient-derived organoid models (n=46). Color coding of histological subtype, vital status, anatomic location, and presence of variant status is described in side panel. Percentage and data bar indicate prevalence of mutation in this cohort as well as The Cancer Genome Atlas (TCGA) pancreatic cancer cohort (n=179). KRAS, TP53, SMAD4, and CDKN2A were most frequently mutated in this cohort, in alignment with the main four driver mutations found in PDAC, as well as the TCGA cohort. Some models had mutations in alternate oncogenic driver genes including GNAS, BRAF, and CTNNB1 (not shown), or less common mutations compared with the TCGA cohort such as BRCA1/2, APC, and ATM. Highlighted models (n=4) were selected for subsequent drug response experiments due to variations in KRAS status: no mutation (n=1), G12D (n=2), or G12V (n=1).

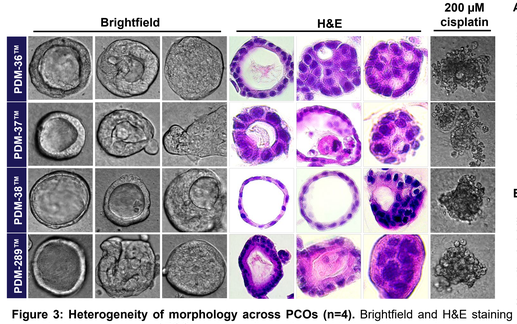

Figure 3: Heterogeneity of morphology across PCOs (n=4). Brightfield and H&E staining reveal typical morphology of PCOs during routine culture, exhibiting either a cystic appearance with defined lumens or without a central lumen. Last column shows impact of toxicity from positive control (200 µM cisplatin) as shown by a loss of structure and cellular organization.

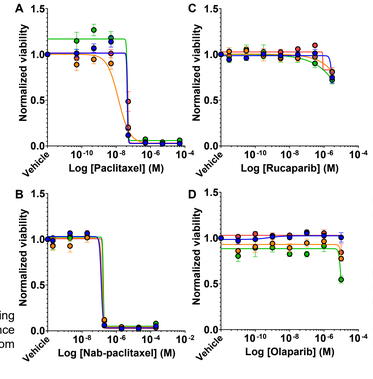

Figure 4: Toxicity induced by taxanes and PARP inhibitors after 168h exposure. Data from other timepoints not shown. (A) Paclitaxel and (B) albumin bound nab-paclitaxel caused similar high toxicity in all models. The PARP inhibitors (C) rucaparib, (D) olaparib, and (E) PJ34 exhibited similar toxicity and potency in all models. PDM-36™ (●), PDM-37™ (●), PDM-38™ (●), PDM-289™ (●)

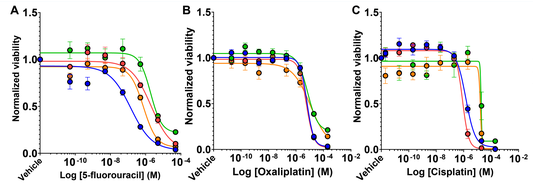

Figure 5: Toxicity induced by 5-FU or platinum-based compounds after 168h exposure. Data from other timepoints not shown. (A) 5-fluorouracil, (B) oxaliplatin, and (C) cisplatin showed similar high toxicity in all models. PDM-36™ (●), PDM-37™ (●), PDM-38™ (●), PDM-289™ (●)

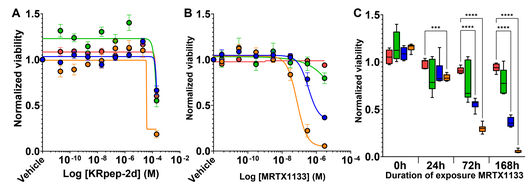

Figure 6: Toxicity by KRAS targeting inhibitors. (A) KRpep-2d exhibited moderate toxicity in all models after 168h at the highest dose. (B) MRTX1133 exhibited differential toxicity at 168h with KRAS G12D variants exhibiting greater toxicity at all three timepoints while (C) an alternate KRAS variant, G12V, exhibited no significant toxicity. Pairwise comparisons with Dunnett's multiple comparisons test. ***P ≤ 0.001. ****P ≤ 0.0001. PDM-36™ (●), PDM-37™ (●), PDM-38™ (●), PDM-289™ (●)

Table 2: Z' Factor scores from drug response assays. Calculated from six separate biological replicates. Calculated from vehicle (negative control) and 200 µM cisplatin (positive control) after 168h exposure.

	Z'
Run 1	0.91
Run 2	0.65
Run 3	0.66
Run 4	0.95
Run 5	0.64
Run 6	0.50
Average	**0.72**

Table 3: Summary of IC_{50} values (µM) after 168h exposure. The highest dose tested is reported if the IC_{50} value could not be calculated.

Higher potency / Lower potency

	paclitaxel	nab-paclitaxel	MRTX1133	rucaparib	5-fluorouracil	oxaliplatin	cisplatin	olaparib	PJ34	KRpep-2d
PDM-36™ KRAS G12D	0.04	0.13	0.34	>3	1.44	6.24	1.44	>10	18.62	>200
PDM-37™ KRAS G12D	0.01	0.15	0.07	>3	7.51	10.85	16.60	>10	9.57	37.85
PDM-38™ KRAS G12V	0.04	0.17	>3	>3	1.91	7.07	18.62	>10	18.57	>200
PDM-289™	0.05	0.17	>3	>3	2.03	5.58	0.82	>10	12.63	>200

Summary and Conclusions

- The HCMI biobank contains organoids from a diverse collection of patients and disease indications, including from pancreatic cancer.
- PCOs from the HCMI have canonical mutations in key genes (KRAS, TP53, SMAD4, and CDKN2A) seen in patient populations and existing large cancer datasets such as the TCGA.
- We used PCOs to validate a viability screening assay with a panel of 10 anti-cancer drugs.
- PCOs exhibited variable drug toxicity that may be in part a consequence of genotype.
- Learn more at www.atcc.org/hcmi & www.atcc.org/organoids

Acknowledgements and References

We would like to acknowledge all founders and contributors to the HCMI: The National Cancer Institute, the National Institutes of Health, Cancer Research UK, Wellcome Sanger Institute, foundation Hubrecht Organoid Technology, Broad Institute, Cold Spring Harbor Laboratory, Stanford University, Weill Cornell Medical College, University of Verona, and the Hubrecht Institute. The models and some data are from the HCMI: www.cancer.gov/ccg/research/functional-genomics/hcmi; dbGaP accession number phs001486.

- Clinton JM and McWilliams-Koeppen P. Initiation, Expansion, and Cryopreservation of Human Primary Tissue-Derived Normal and Diseased Organoids in Embedded Three-Dimensional Culture. Curr Protoc Cell Bio 82(1): e66, 2019.
- Hallin J, et al. Anti-tumor efficacy of a potent and selective non-covalent KRASG12D inhibitor. Nat Med 28(10): 2171-2182, 2022.

ATCC 10801 University Boulevard, Manassas, Virginia 20110-2209 **Phone:** 800.638.6597 **Email:** SalesRep@atcc.org **Web:** www.atcc.org